Journal of Molecular Structure 1081 (2015) 375–380

Contents lists available at ScienceDirect

Journal of Molecular Structure

journal homepage: www.elsevier.com/locate/molstruc

Solvent effect in keto–enol tautomerism for a polymerizable β-ketonitrile monomer. Spectroscopy and theoretical study

Juan M. Giussi [a,b], Belén Gastaca [b], Martín J. Lavecchia [c], Mercedes Schiavoni [b], M. Susana Cortizo [a,b], Patricia E. Allegretti [b,*]

[a] Instituto de Investigaciones Fisicoquímicas Teóricas y Aplicadas (INIFTA), CCT-La Plata, Facultad de Ciencias Exactas, Universidad Nacional de La Plata, 1900 La Plata, Argentina
[b] Laboratorio de Estudio de Compuestos Orgánicos (LADECOR), Facultad de Ciencias Exactas, Universidad Nacional de La Plata, 1900 La Plata, Argentina
[c] Centro de Química Inorgánica (CEQUINOR), CCT-La Plata, Facultad de Ciencias Exactas, Universidad Nacional de La Plata, 1900 La Plata, Argentina

HIGHLIGHTS

- A beta-ketonitrile studied by NMR spectroscopy and DFT methods.
- Experimental and calculated NMR chemical shifts showed good correlation.
- Enol content increases with solvent polarity.

GRAPHICAL ABSTRACT

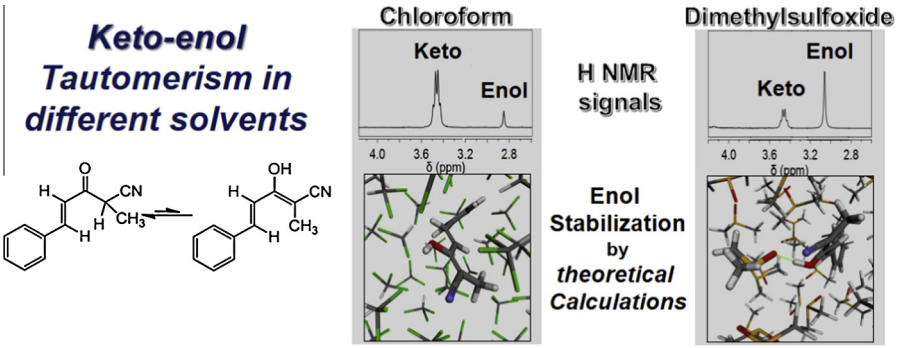

ARTICLE INFO

Article history:
Received 9 September 2014
Received in revised form 20 October 2014
Accepted 21 October 2014
Available online 31 October 2014

Keywords:
β-Ketonitrile
2-Methyl-5-phenyl-3-oxo-4-pentenenitrile
Tautomeric equilibria
NMR spectrometry
DFT calculations

ABSTRACT

The beta-ketonitrile 2-methyl-5-phenyl-3-oxo-4-pentenenitrile, a polymerizable monomer, exists in two important tautomeric forms, keto and enol isomers. This compound has been studied as monomer in polymerization reactions and the resulting polymers have been applied in fields of nanotechnology. Currently, these are being studied in nanomedicine. To understand the tautomeric equilibrium, we have studied this compound in solution by NMR spectrometry. Correlation with DFT calculations has been carried out in order to understand the system behavior. The results found in this work, both by experiments and calculations, show that the enol content increases with solvent polarity.

Introduction

Tautomerism in organic chemistry has been extensively studied in condensed and gas phase by spectrometric methods on a wide variety of functional groups, such as carbonilic, nitro and nitrile compounds [1-4]. Considering that numerous cellular processes occur through tautomeric forms of certain compounds, tautomerism has become an interesting field of study. For instance, Benner discussed different ways in which organic chemistry can be used to produce artificial DNA molecules that have broad therapeutic applications in diagnostic tests for disease treatment [5]. The presence of tautomeric groups in these molecules is of special importance for that they are discriminated as specific substrates, according to the environment in which they exist and, therefore, could make them interesting in biomedicine.

* Corresponding author. Tel.: +54 221 4243104.
E-mail address: pallegre@quimica.unlp.edu.ar (P.E. Allegretti).

http://dx.doi.org/10.1016/j.molstruc.2014.10.054
0022-2860/

β-Ketonitriles can present many theoretical tautomeric forms as it is shown in Scheme 1 [6,7]. Furthermore, γ,δ-unsaturated β-ketonitriles are an interesting family of these compounds due to their possibility of polymerization. In fact, the studied compound in this work has been copolymerized with styrene. The copolymerization behavior and polymer properties were influenced by tautomeric equilibria [8]. In addition, the synthesized copolymers were nanostructured to obtain nanofibers for biomedical applications [9].

It is well known that computational tools are of great aid to gain insights that could help to understand and predict the structure, stability, and reactivity of organic compounds. Among these, DFT has proven to be very effective. Keto–enol and nitrile–ketenimine equilibria of the analyzed compound in the present work, were previously studied by mass spectrometry [10]. A good correlation was found in enthalpy changes obtained experimentally and by density functional theory (DFT) calculations, in which the ketonitrile tautomer was favoured. In a previous work, the kinetic and thermodynamic parameters of tautomerization were calculated. Moreover, the calculated chemical shifts are in agreement with the experimental data obtained by ^{1}H NMR and ^{13}C NMR data in the study of 6-benzoylmethyl-1,3,5-triazin-2,4-diamine [11].

Additionally, solvent effects on tautomeric equilibria in several β-ketonitriles have been investigated using nuclear magnetic resonance (NMR) spectroscopy and theoretical methods [12]. The experimental chemical shifts were compared with theoretical values obtained by using gauge-including atomic orbital (GIAO) calculations, implemented at DFT.

The main objective of this work is the study of tautomerism in solution by NMR spectrometry. IR spectroscopy and Gas-Chromatography–Mass spectrometry are also used in order to identify the compound. Furthermore, a correlation between experimental and theoretical results was found. The analysis of these simple structures may help to correlate their reactivity with the chemical behavior of complex systems, like polymers.

Experimental

Materials

Propionitrile (99.0%, Fluka), Diisopropylamine (99%, Aldrich), Bultyllithium (1.6 M in hexane, Aldrich), Cinnamaldehyde (98%, Carlo Erba), Chromium Trioxide–Dipyridine Complex (synthesized according to literature technique [13]).

Synthesis

2-Methyl-5-phenyl-3-oxo-4-pentenenitrile was obtained through an adaptation of a method previously described [14,15], using a γ-δ unsaturated β-hydroxynitrile as intermediate product, which was later oxidized to obtain the γ-δ unsaturated β-ketonitrile. The product was identified by Gas-Chromatography–Mass spectrometry, ^{1}H and ^{13}C NMR and FT-IR spectroscopy. Structural studies have been carried out; the compound is stable in absence of polymerization initiator.

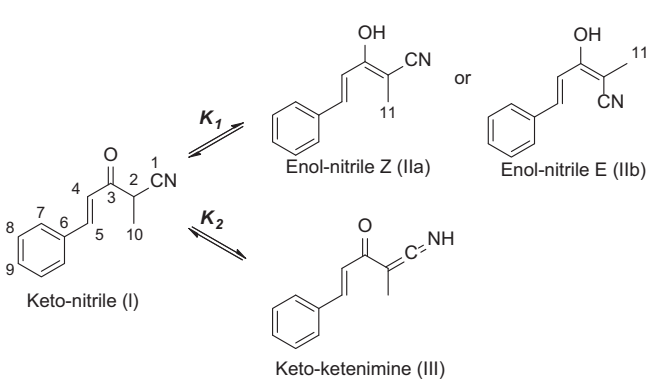

Scheme 1. Keto–enol and nitrile–ketenimine equilibria for 2-methyl-5-phenyl-3-oxo-4-pentenenitrile.

Structural determinations

^{1}H NMR and ^{13}C NMR spectrometry

^{1}H NMR and ^{13}C NMR spectra of the studied compound were registered with a Varian Mercury Plus Spectrometer, 200 MHz. Toluene-d_8, chloroform-d_1, tetrahydrofuran-d_8, acetonitrile-d_3 and dimethylsulfoxide-d_6 were used as solvents. The spectral conditions were, as follows: width 3201 Hz, acquisition time 4.09 s and 8–16 scans per spectrum. Digital resolution was 0.39 Hz per point. Deuterated solvents were used and tetramethylsilane (TMS) was the internal standard. The sample concentration was 0.41 wt% and the spectra were recorded at room temperature.

Computational methods

The conformational space of the starting conformations (Scheme 1) was explored using genetic algorithm as implemented in Balloon software using the Merck molecular force field (MMFF94) and default parameters [16]. The generated geometries were then preoptimized with semiempirical PM6 [17] method using MOPAC package [18]. This step helps to achieve faster convergence in comparison to using more expensive methods directly.

The PM6-optimized geometries were further optimized using tools from the density functional theory [19–21] as implemented in the Gaussian 03 package [22]. Only those optimized geometries lying up to 3 kcal mol^{-1} above the lowest-energy conformer of every tautomer were considered for further studies. The energy threshold of 3 kcal mol^{-1} provides some confidence that the contribution of higher energy conformations is less than 1% to every property measured at 298.15 K, according to the Maxwell–Boltzmann distribution.

The optimizations are accomplished using the Becke's three parameters hybrid density functional [23] with the gradient-corrected correlation functional due to Lee et al. [24], B3LYP method [25]. 6-311++G** basis set was used.

The Hessian matrix was calculated at the same level of theory and it was diagonalized for all the optimized geometries to verify whether they were local minima or saddle points on the potential energy surface of the molecules. These calculations were also carried out with the Gaussian 03 package.

Solvent effects on the conformational behavior of the studied compound were analyzed in two ways: implicit solvent through the integral formalism model (IEFPCM) on B3LYP/6-311++G** optimized structures with B3LYP/6-311++G** and PBE0/6-31G* model chemistries with UFF and UAKS radii, respectively [26,27]; and explicit solvent, employing Packmol [28] software to surround the conformers with a sphere of solvent molecules with radius 10 Å, and then minimized with PM6 semiempirical method. The last calculation was done to analyze qualitatively interactions between 2-methyl-5-phenyl-3-oxo-4-pentenenitrile and solvent molecules. To estimate the Gibbs free energy of a tautomer conformer employing IEF-PCM model, the following equation was used:

$$G_{soln} = G_{gas} + \Delta G_{solv} \quad (1)$$

G_{soln} refer to the Gibbs free energy in solution-phase, G_{gas} estimated as sum of electronic and thermal free energies (output from a frequency calculation), and ΔG_{solv} solvation free energy estimated as:

$$\Delta G_{solv} \approx E_{soln} - E_{gas} \quad (2)$$

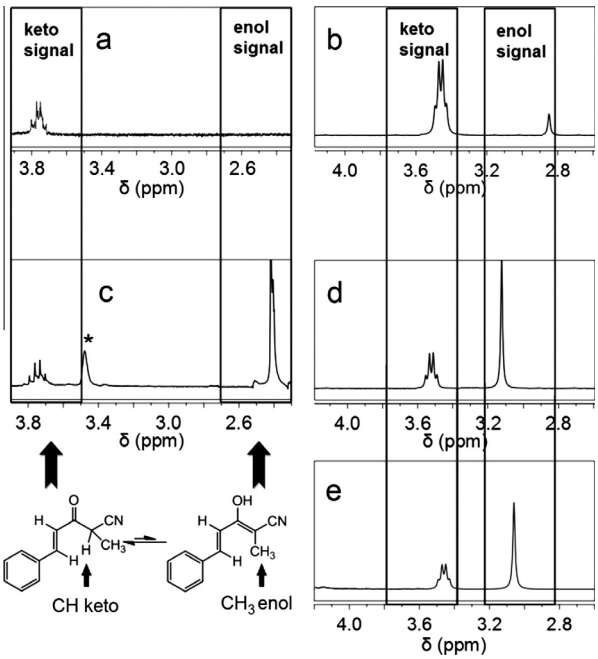

Fig. 1. ^{1}H NMR spectra (extended zone between 2 and 4 ppm) for 2-methyl-5-phenyl-3-oxo-4-pentenenitrile in (a) toluene, (b) chloroform, (c) tetrahydrofuran, (d) acetonitrile and (e) dimethylsulfoxide. *Solvent signal.

Table 1
Enol molar fraction (x_{enol}), keto molar fraction (x_{keto}) and tautomeric constant (K_T) of 2-methyl-5-phenyl-3-oxo-4-pentenenitrile in different solvents.

Solvent	x_{enol}	x_{keto}	$K_T = x_{enol}/x_{keto}$
Toluene-d_8	0.000*	1.000	0.000
$CDCl_3$	0.041	0.959	0.005
THF-d_8	0.161	0.839	0.192
ACN-d_3	0.289	0.711	0.406
DMSO-d_6	0.358	0.642	0.558

* In toluene, the enol signal does not appear in the spectrum.

where E_{soln} and E_{gas} are the electronic energy of the conformer in the presence and absence of the continuum solvent field, respectively, calculated on conformations optimized in the gas phase. In this work, we are interested in calculating the difference ΔG_{soln} instead of absolute free energies, in order to estimate the relative stability between two species. In this way, there are error compensations.

^{1}H and ^{13}C isotropic shielding tensors were calculated using the Gauge-Including Atomic Orbital method [30,31] as implemented in the Gaussian 03 package. C-PCM model was used to simulate acetonitrile effects. The isotropic shieldings are turned into chemical shifts by two methods: subtracting the corresponding isotropic shieldings of tetramethylsilane (TMS), which are calculated at the same level of theory, and using scaling factors [29] (compiled in cheshirenmr.info).

Results and discussion

Scheme 1 shows the theoretical tautomeric equilibria present for the β-ketonitrile studied: the keto–enol tautomerism through the keto-nitrile (I) and enol (E and Z)-nitrile (II) forms and nitrile–ketenimine tautomerism through the keto-nitrile (I), keto-ketenimine (III) forms. The existence of all these tautomeric forms in the gas phase has been previously demonstrated by CG-MS [10]. The nitrile–ketenimine equilibrium could not be observed by ^{1}H NMR spectrometry, due to the lower sensitivity of this method and the low proportion of keto-ketenimine form (see Correlation with theoretical calculations section) [32].

The tautomeric equilibrium between (I) and (II) tautomers was studied by ^{1}H NMR using solvents of different polarity (toluene, chloroform, tetrahydrofuran, acetonitrile and dimethylsulfoxide). Analysis of keto–enol equilibrium by ^{1}H NMR consists of taking certain nucleus as a reference, in which chemical displacement changes substantially, depending on the tautomeric form considered. Fig. 1 shows the ^{1}H NMR spectra (extended zone between 2 and 4 ppm) for 2-methyl-5-phenyl-3-oxo-4-pentenenitrile in the five solvents, together with the assignment of signals for the keto-nitrile (I) and enol-nitrile (II) forms. It must be noted that this methodology does not allow distinguishing between the geometric isomers (IIa and IIb), and thus these equilibria were not evaluated individually.

The rate of keto–enol interconversion is sufficiently slow on the NMR time scale to allow the calculation of the tautomeric equilibrium constant ($\boldsymbol{K_1}$) from the areas (I), obtained by integration of the selected peaks on each spectrum. Thus, the signals at $\delta = 2.85$, 2.42, 3.12 and 3.06 ppm were assigned to the methyl hydrogen of enol-nitrile (II) form in chloroform, tetrahydrofuran, acetonitrile and dimethylsulfoxide, respectively. The corresponding signal in toluene was not observed. On the other hand, the signals at $\delta = 3.74$, 3.45, 3.73, 3.51 and 3.45 ppm were assigned to the methine hydrogen of keto-nitrile (I) tautomeric form in toluene, chloroform, tetrahydrofuran, acetonitrile and dimethylsulfoxide, respectively. In order to obtain K_T, it is necessary to divide the value of the integral ratio of the peaks of both tautomeric forms (I_{keto} and I_{enol}) by the number of hydrogen atoms for which integrates, using Eq. (3). Table 1 presents the x_{enol} $\left(x_{enol} = \frac{I_{enol}/3}{\frac{I_{enol}}{3}+I_{keto}}\right)$ and K_T values for 2-methyl-5-phenyl-3-oxo-4-pentenenitrile in the analyzed solvents. As can be seen, x_{enol} and K_T grow as the polarity of the solvents increases, suggesting a higher stabilization of the enol tautomeric form in more polar solvents.

$$K_T = \frac{I_{enol}/3}{I_{keto}} \tag{3}$$

In order to quantify the behavior of keto–enol tautomerism in solution, Kamlet–Taft linear solvation energy relationship has been carried out. [33]

$$XYZ = XYZ_0 + s\pi^* + a\alpha + b\beta \tag{4}$$

In Eq. (4), XYZ is the property to be correlated, XYZ_0 is the property related to a standard process, π^* is the dipolarity/polarizability

Table 2
Differences in Gibbs free energy ΔG (in kcal mol^{-1}) relative to the most stable conformation for 2-methyl-5-phenyl-3-oxo-4-pentenenitrile calculated with IEF-PCM implicit solvent model using B3LYP/6-311++G** and UFF radii, and PBE0/6-31G* and radii UAKS, in parentheses.

Tautomeric form solvent	Keto-nitrile (I)	Enol-nitrile Z (IIa)	Enol-nitrile E (IIb)	Keto-ketenimine (III)
Gas phase	0.0	2.9	3.8	13.4
Toluene ($\varepsilon = 2.3741$)	0.0 (0.0)	3.5 (3.1)	3.6 (2.9)	13.7 (12.7)
$CHCl_3$ ($\varepsilon = 4.7113$)	0.0 (0.0)	3.7 (2.9)	3.5 (2.1)	13.7 (11.9)
THF ($\varepsilon = 7.4257$)	0.0 (0.0)	3.8 (2.7)	3.4 (1.8)	13.7 (11.5)
ACN ($\varepsilon = 35.688$)	0.0 (0.0)	4.0 (2.5)	3.4 (1.3)	13.7 (10.9)
DMSO ($\varepsilon = 46.826$)	0.0 (0.0)	4.1 (2.4)	3.4 (1.2)	13.7 (10.9)

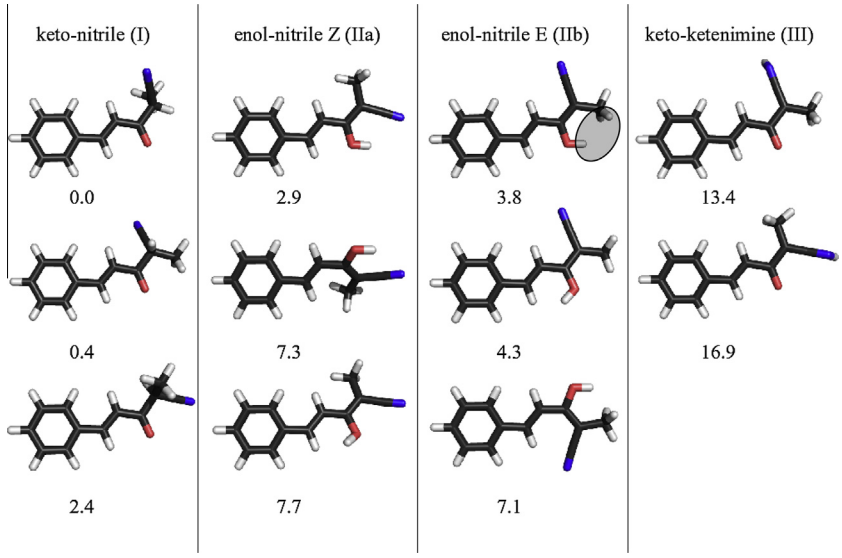

Fig. 2. Structures of the most stable conformations, and ΔG (in kcal mol^{-1}) calculated in the gas phase relative to the most stable. * highlighted the repulsive interaction in gas phase for enol-nitrile E (IIb).

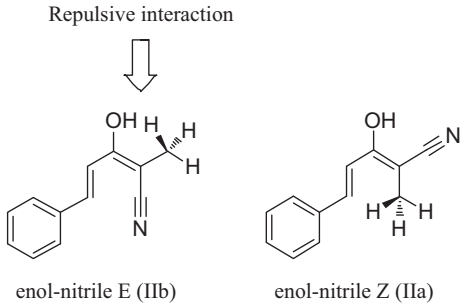

Fig. 3. Representation of repulsive interaction between OH group and the H-methylic in enol-nitrile Z (IIb).

Table 3
Comparison between experimental and calculated ^{13}C NMR and ^{1}H NMR chemical shifts in Chloroform for 2-methyl-5-phenyl-3-oxo-4-pentenenitrile. The isotropic shieldings are turned into chemical shifts by subtracting the corresponding isotropic shieldings of tetramethylsilane (TMS). B3LYP/6-311++G**/GIAO(scrf)//B3LYP/6-311++G**(gas).

C/H	Exp δ_C	Calc δ_C	Exp δ_H	Calc δ_H
1	124.6	118.1	–	–
2	36.5	41.2	3.2	4.4
3	192.3	190.3	–	–
4	117.9	115.2	7.8	8.0
5	146.7	145.9	7.1	8.3
6	134.0	131.9	–	–
7	128.1	128.0	7.9	8.2
8	129.0	126.4	7.5	7.9
9	129.5	129.8	7.6	8.0
10	17.7	17.3	1.7	1.5
11	–	–	2.9	2.0
R^2		0.9977		0.9519
RMSE		2.6262		0.6963

See assignment in Scheme 1.

term, α is the hydrogen-bond donating (HBD) capacity and β is the hydrogen-bond accepting (HBA) capacity. The coefficient of the individual interaction contributions can be determined by using multiple linear correlation analysis. The solvatochromic parameters π*, α and β of different solvents for the square multiple correlation analysis were tabulated for Kamlet et al. [33] Through this equation, it was possible to relate the keto molar fraction (x_{keto}) with solvatochromic parameters of different solvents. The α parameter was vanished because none of the solvents has hydrogen bond donating power. The regression analysis gave a good linear correlation, according to Eq. (5).

$$\ln x_{keto} = 0.408 - 1.35\pi^* + 0.27\beta \quad (5)$$

$n = 5$, $r = 0.986$ SD = 0.009.

In the correlation, n is the number of solvents, r the correlation coefficients and SD the standard deviation. The term that accomplishes to π* is more important than the β term, suggesting that the solute–solvent dipole–dipole interactions occur preferably.

Correlation with theoretical calculations

The differences in Gibbs free energy ΔG among most stable conformations of keto-nitrile, enol-nitrile and keto-ketenimine in the gas phase for 2-methyl-5-phenyl-3-oxo-4-pentenenitrile are shown in Table 2. Fig. 2 shows selected conformations of the tautomers optimized in the gas phase. Some conformations, which ΔG exceed 3 kcal mol^{-1}, are also included for illustrative purposes (structures available in Supplementary Material).

Table 2 also shows the ΔG calculated in implicit solvents. According to the data obtained, keto-nitrile form appears to be the most stable tautomer. Moreover, the enolic tautomers have similar ΔG and the less stable structure corresponds to keto-ketenimine form.

As it is shown in Table 2, in gas phase the enol-nitrile Z (IIa) tautomer is more stable than the enol-nitrile E (IIb), indicating a possible repulsive interaction between the methyl group and the *OH group* in enol-nitrile E (IIb) isomer, as depicted in Fig. 3, see it also highlighted in Fig. 2.

In solution, the order is inverted and the difference between ΔG enol-nitrile Z and ΔG enol-nitrile E increases with increasing polarity of the solvent with both theoretical methods, IEF-PCM implicit solvent model using B3LYP/6-311++G** and UFF radii, and PBE0/6-31G* and radii UAKS, in parentheses. These results indicate a relevant solute–solvent interaction. The differences between ΔG enol-nitrile and ΔG keto-nitrile decrease with increasing polarity

Table 4
Comparison between experimental and calculated ^{13}C NMR and ^{1}H NMR chemical shifts in Chloroform for 2-methyl-5-phenyl-3-oxo-4-pentenenitrile. The isotropic shieldings are turned into chemical shifts using scaling factors [29] (compiled in cheshirenmr.info) mPWPW91/6-311+G(2d,p)/GIAO(scrf) // B3LYP/6-311+G(2d,p)(gas).

C/H	Exp δ_C	Calc δ_C	Exp δ_H	Calc δ_H
1	124.6	124.6	–	–
2	36.5	42.1	3.2	4.3
3	192.3	192.6	–	–
4	117.9	118.6	7.8	7.4
5	146.7	149.9	7.1	8.0
6	134.0	133.4	–	–
7	128.1	131.1	7.9	7.9
8	129.0	129.3	7.5	7.6
9	129.5	133.6	7.6	7.6
10	17.7	17.0	1.7	1.6
11	–	–	2.9	2.0
R^2		0.9982		0.9442
RMSE		2.3054		0.6996

See assignment in Scheme 1.

of the solvent and are in agreement with the experimental results, where the more polar solvents favor the enol forms, without discriminating between E or Z tautomer.

It can also be seen in the table that the tendency in the decrease of ΔG (or increment of K_T, estimated by $K_T = e^{(-\Delta G/RT)}$), studied experimentally (see Table 1) and by PBE0/6-31G* model chemistry with solvent effects, is the same. It must be noticed, however, that the calculated tendency is less pronounced that the experimental and should be treated in a qualitative manner. On the other hand, this tendency for B3LYP/6-311++G** model chemistry is accomplished only for Z tautomer.

Calculated dipole moments can help us to interpret what is observed experimentally. The values of this parameter for keto-nitrile, enol-nitrile E, and enol-nitrile Z in the gas phase are 3.34D, 4.26D, 4.99D respectively, employing the B3LYP/6-311++G** model chemistry. This tendency ($\mu_{keto\text{-}nitrile} < \mu_{enol\text{-}nitrile\ E} < \mu_{enol\text{-}nitrile\ Z}$) is conserved in implicit solvent field and using the PBE0/6-31G* model chemistry. Those species that have higher dipole moments are stabilized in more polar solvents. This proposal is in agreement with the result obtained by Kamlet–Taft linear solvation energy relationship, Eq. (5), where we said that the term π^* (dipolarity/polarizability) is the most relevant. Then, the enol forms are more stable than keto form with increasing solvent polarity. Furthermore, we can explain stabilization of enol-nitrile Z respect to enol-nitrile E, showed by calculation, based on the same argument. The latter was not tested experimentally, since the techniques used do not discriminate between the different forms of enol tautomer.

In order to correlate more experimental parameters with theoretical calculations, Tables 3 and 4 present the experimental and calculated chemical shift values of ^{13}C NMR and ^{1}H NMR and Fig. 4 shows the correlation between them.

^{13}C NMR correlation (Fig. 4a) shows excellent agreement and all values correspond to ketonitrile tautomer. Moreover, good correlation is obtained for ^{1}H NMR (Fig. 4b). However, a discrepancy is present in the tautomeric H, the value 2.9 ppm for the methyl enolic group (11) is compared with 2.0 ppm obtained by theoretical methods and the experimental value 3.2 ppm for the methinic keto group (2) is compared with the calculated 4.4 ppm. The discrepancy has been attributed to the exchangeable character of tautomeric hydrogen nucleus, the theoretical methods minimize the solvent interaction of methyl group (11) moving at higher fields (minor δ value) and maximize the solvent interaction of methinic keto group (2) moving at minor fields (higher δ value).

In order to understand the behavior of the system, Fig. 4 represents the established interaction between the enolic hydrogen and

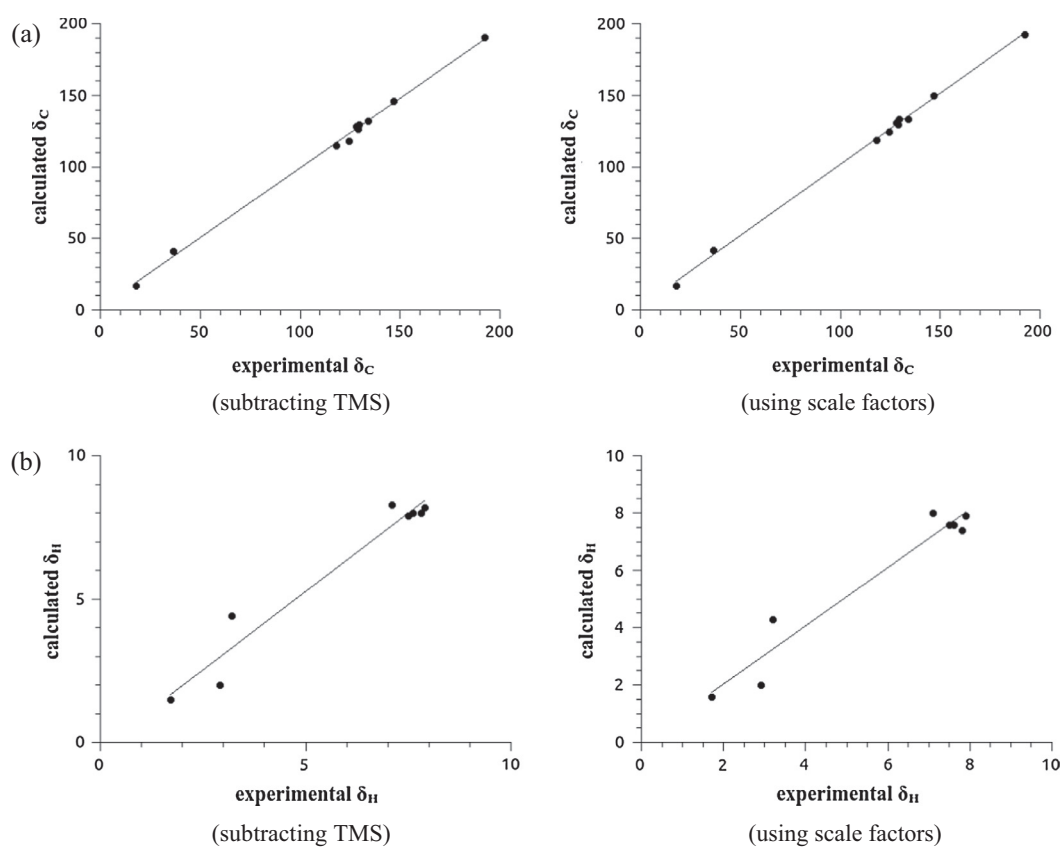

Fig. 4. Correlation of experimental and calculated results of (a) ^{13}C NMR and (b) ^{1}H NMR, in chloroform for 2-methyl-5-phenyl-3-oxo-4-pentenenitrile.

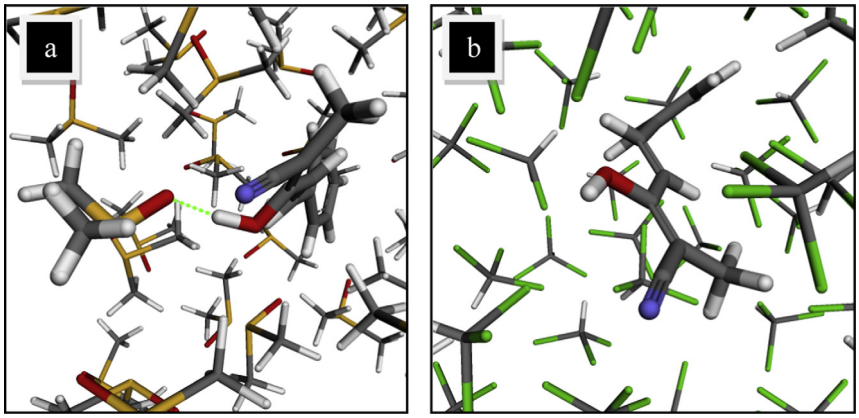

Fig. 5. Graphical representation of interaction between (a) enolic H and DMSO solvent (b) enolic H and $CHCl_3$ solvent.

the oxygen of DMSO obtained by PM6 calculations (solvent with mayor value of β, $\beta = 0.76$) (Fig. 5a). As this interaction is not possible in $CHCl_3$ (solvent with minor value of β, $\beta = 0$), the molecular disposition is different (Fig. 5b). This result is in agreement with the observed experimental behavior.

Another discrepancy was observed in hydrogen nucleus 5, the rotation in the bond between C(3) and C(4) (see Scheme 1) give conformations with very different interactions of this hydrogen. For example, in Fig. 2, the less stable conformation of enol-nitrile Z (IIa) (7.7 kcal mol^{-1}) and the second conformation of enol-nitrile E (IIb) (4.3 kcal mol^{-1}), structures with the H of OH close to H (5), the theoretical chemical shifts is 7.1, equal of experimental value.

The results of this study showed an interesting correlation between experimental and theoretical data. The combination of these have allowed to predict structural stabilities.

Conclusion

Keto–enol equilibrium in 2-methyl-5-phenyl-3-oxo-4-pentene-nitrile was studied by spectrometric and theoretical methods. A good correlation for the behavior in solution was found between NMR data and DFT calculations. The results displayed that the increase in solvent polarity increases the enol content.

A correlation with solvent parameters has been carried out. The most important parameter in the displacement of tautomeric keto–enol equilibrium is the term that accomplishes to π^* in Kamlet correlation, indicating that solute–solvent dipole–dipole interactions predominate. This result is also in agreement with DFT calculations.

The comparison between experimental and calculated ^{13}C NMR and ^{1}H NMR chemical shifts showed a good correlation with some discrepancies in the tautomeric hydrogen nucleus. This could be by the fact that the theoretical methods used minimize the solvent interaction with certain nuclei and maximize others.

Appendix A. Supplementary material

Supplementary data associated with this article can be found, in the online version, at http://dx.doi.org/10.1016/j.molstruc.2014.10.054. These data include MOL files and InChiKeys of the most important compounds described in this article.

References

[1] P.I. Nagy, K. Takacs-Novak, Phys. Chem. Chem. Phys. 6 (2004) 2838.
[2] P.E. Allegretti, M.M. Schiavoni, M.S. Cortizo, E.A. Castro, J.J.P. Furlong, Int. J. Mol. Sci. 5 (2004) 294.
[3] E.D. Raczynska, W. Kosinska, B. Osmialowski, R. Gawinecki, Chem. Rev. 105 (2005) 3561.
[4] D.L. Ruiz, M.M. Schiavoni, S.L. Laurella, J.M. Giussi, J.J.P. Furlong, P.E. Allegretti, Spectrochim. Acta – Part A: Mol. Biomol. Spectrosc. 78 (2011) 1397.
[5] S.A. Benner, Science 306 (2004) 625.
[6] D.L. Ruiz, J.M. Giussi, A. Albesa, M. Schiavoni, J. Furlong, P. Allegretti, Spectrochim. Acta – Part A: Mol. Biomol. Spectrosc. 77 (2010) 485.
[7] Z. Rappoport, The Chemistry of the Cyano Group, Interscience Publishers, London, 1970.
[8] J.M. Giussi, P.E. Allegretti, M.S. Cortizo, J. Polym. Sci. – Part A: Polym. Chem. 50 (2012) 4161.
[9] J.M. Giussi, I. Blaszczyk-Lezak, P.E. Allegretti, M.S. Cortizo, C. Mijangos, Polymer 54 (2013) 5050.
[10] J.M. Giussi, B. Gastaca, A. Albesa, M.S. Cortizo, P.E. Allegretti, Spectrochim. Acta – Part A: Mol. Biomol. Spectrosc. 78 (2011) 868.
[11] N. Sachdeva, A.V. Dolzhenko, W.K. Chui, C. R. Chim. 14 (2011) 580.
[12] D.L. Ruiz, A.G. Albesa, A. Ponzinibbio, P.E. Allegretti, M.M. Schiavoni, J. Phys. Org. Chem. 23 (2010) 985.
[13] R.W. Ratcliffe, Org. Synth. 55 (1976) 84.
[14] R. Zibuck, J. Streiber, Org. Synth. 71 (1993) 236.
[15] J.C. Collins, W.W. Hess, Org. Synth. 52 (1972) 5.
[16] M.J. Vainio, M.S. Johnson, J. Chem. Inf. Model. 47 (2007) 2462.
[17] J.J.P. Stewart, J. Mol. Model. 13 (2007) 1173.
[18] MOPAC2009, James J.P. Stewart, Stewart Computational Chemistry, Colorado Springs, CO, USA, 2008, HTTP://OpenMOPAC.net.
[19] P. Hohenberg, W. Kohn, Phys. Rev. 136 (1964) B864.
[20] W. Kohn, L.J. Sham, Phys. Rev. 140 (1965) A1133.
[21] R. Parr, W. Yang, Density Functional Theory of Atoms and Molecules, Oxford University Press, 1989.
[22] M.J. Frisch, G.W. Trucks, H.B. Schlegel, G.E. Scuseria, M.A. Robb, J.R. Cheeseman, J.A. Montgomery, Jr., T. Vreven, K.N. Kudin, J.C. Burant, J.M. Millam, S.S. Iyengar, J. Tomasi, V. Barone, B. Mennucci, M. Cossi, G. Scalmani, N. Rega, G.A. Petersson, H. Nakatsuji, M. Hada, M. Ehara, K. Toyota, R. Fukuda, J. Hasegawa, M. Ishida, T. Nakajima, Y. Honda, O. Kitao, H. Nakai, M. Klene, X. Li, J.E. Knox, H.P. Hratchian, J.B. Cross, V. Bakken, C. Adamo, J. Jaramillo, R. Gomperts, R. E. Stratmann, O. Yazyev, A. J. Austin, R. Cammi, C. Pomelli, J.W. Ochterski, P.Y. Ayala, K. Morokuma, G.A. Voth, P. Salvador, J.J. Dannenberg, V.G. Zakrzewski, S. Dapprich, A.D. Daniels, M.C. Strain, O. Farkas, D. K. Malick, A.D. Rabuck, K. Raghavachari, J. B. Foresman, J.V. Ortiz, Q. Cui, A.G. Baboul, S. Clifford, J. Cioslowski, B. B. Stefanov, G. Liu, A. Liashenko, P. Piskorz, I. Komaromi, R.L. Martin, D.J. Fox, T. Keith, M.A. Al-Laham, C.Y. Peng, A. Nanayakkara, M. Challacombe, P.M.W. Gill, B. Johnson, W. Chen, M.W. Wong, C. Gonzalez, J.A. Pople, Gaussian 03, revision d.01 [computer software], 2004.
[23] A. Becke, J. Chem. Phys. 98 (1993) 5648.
[24] C. Lee, W. Yang, R.G. Parr, Phys. Rev. B 37 (1988) 785.
[25] P. Stephens, F. Devlin, C. Chabalowski, M. Frisch, J. Phys. Chem. 98 (1994) 11623.
[26] B. Mennucci, E. Cancès, J. Tomasi, J. Phys. Chem. B 101 (1997) 10506.
[27] J. Tomasi, B. Mennucci, E. Cancès, J. Mol. Struct. (Theochem) 464 (1999) 211.
[28] L. Martínez, R. Andrade, E.G. Birgin, J.M. Martínez, J. Comput. Chem. 30 (2009) 2157.
[29] M.W. Lodewyk, M.R. Siebert, D.J. Tantillo, Chem. Rev. 112 (2012) 1839–1862.
[30] R. Ditchfield, Mol. Phys. 27 (1974) 789–807.
[31] K. Wolinski, J.F. Hinton, P. Pulay, J. Am. Chem. Soc. 112 (1990) 8251–8260.
[32] J.M. Giussi, A. Ponzinibbio, M.S. Cortizo, P.E. Allegretti, Spectrochim. Acta A: Mol. Biomol. Spectrosc. 77 (2010) 367.
[33] M.J. Kamlet, J.L.M. Abboud, M.H. Abraham, R.W. Taft, J. Org. Chem. 48 (1983) 2877.